

# Charging of Quantum Dots by Sulfide Redox Electrolytes Reduces Electron Injection Efficiency in Quantum Dot Sensitized Solar Cells

Haiming Zhu, Nianhui Song, and Tianquan Lian\*

Department of Chemistry, Emory University, Atlanta, Georgia 30322, United States

**S** Supporting Information

**ABSTRACT:** In quantum dot (QD) sensitized solar cells (QDSSCs), redox electrolytes act as hole scavengers to regenerate the QD ground state from its oxidized form, thus enabling a continuous device operation. However, unlike molecular sensitizers, QDs also have redox-active trap states within the band gap, which can be charged in the presence of redox electrolyte. The effects of electrolyte induced charging of QDs on the performance of QDSSCs have not been reported. Here, using steady-state and time-resolved absorption and emission spectroscopy, we show that CdSe/CdS<sub>3ML</sub>ZnCdS<sub>2ML</sub>ZnS<sub>2ML</sub> core/multishell QDs are charged in the presence of sulfide electrolytes due to the reduction of surface states. As a result, exciton lifetimes in these QDs are shortened due to an Auger recombination process. Such charging induced fast Auger recombination can compete effectively with electron transfer from QDs to TiO<sub>2</sub> and reduce the electron injection efficiency in QDSSCs. We believe that the reported charging effects are present for most colloidal nanocrystals in the presence of redox media and have important implications for designing QD-based photovoltaic and photocatalytic devices.

Because of their unique optoelectronic properties and low cost processing, colloidal quantum-confined semiconductor nanoparticles, or quantum dots (QDs), have been widely investigated as an alternative to molecular dyes in sensitized solar cells.<sup>1,2</sup> More recently, this interest has been intensified due to the possibility of multiexciton and hot carrier extraction from QDs, which can potentially improve the efficiency of QD sensitized solar cells (QDSSCs).<sup>3,4</sup> The operation of QDSSCs involves many processes, including electron injection from photoexcited sensitizers to oxide electrodes, hole filling by redox electrolytes and carrier transport, and charge collection at the electrodes. Hole filling by redox electrolytes in QDSSCs (mostly sulfide/polysulfide,  $-0.45$  V vs NHE<sup>5</sup>) removes the valence band holes in photo-oxidized QDs to regenerate the QD ground state, which prevents QD photocorrosion and enables continuous device operation.<sup>5–8</sup> For molecular sensitizers, the redox electrolyte can be chosen to have a potential that falls within the highest occupied and the lowest unoccupied molecular orbitals, such that it can reduce the oxidized sensitizer and have negligible effect on reduced form. However, unlike molecular sensitizers, QDs also have redox active trap states within the band gap in addition to the conduction (CB) and valence (VB) band states. In working solar cells, in addition to the expected hole

extraction process, the redox electrolyte can also fill these mid-gap states to form charged QDs. The roles of these mid-gap states on charge carrier generation and recombination have been suggested in recent photoelectro- and electrochemical studies of QDSSCs and related devices.<sup>9,10</sup> Previous studies of QD intrinsic carrier relaxation and interfacial charge transfer were typically conducted with either colloidal solutions or dry film samples without redox electrolytes.<sup>6,11–14</sup> It remains unclear how redox electrolyte induced charging of QDs affects their exciton decay and charge transfer dynamics as well as the efficiency of QDSSCs.

In this paper, we employ steady-state and time-resolved absorption and emission spectroscopic methods to investigate the effect of sulfide electrolytes on CdSe based QDs. It has been shown that surface corrosion by sulfide creates a thin CdSe<sub>x</sub>S<sub>1–x</sub> surface layer on core-only CdSe QDs.<sup>8</sup> To avoid the complication caused by surface corrosion, we use a water-soluble type I core/multishell QDs (CdSe/CdS<sub>3ML</sub>ZnCdS<sub>2ML</sub>ZnS<sub>2ML</sub>) capped with carboxylic acid functional group in this study. We show that in the presence of sulfide electrolytes, these QDs are charged, and instead of long-lived single exciton in uncharged QDs, electrolyte charging induced fast Auger recombination greatly reduces the exciton lifetime in these charged QDs. Hole transfer from QDs to sulfide is also observed but is much slower than the Auger recombination process. The electrolyte charging induced fast Auger recombination competes effectively with interfacial electron transfer (ET) process, leading to significant reduction of electron injection efficiency.

QD-S<sup>2–</sup> solution was prepared by mixing 0.01 M Na<sub>2</sub>S solution with water-soluble QDs in dark (see S11 for experiment details). Because of hydrolysis, a large portion of the sulfide ions is in the SH<sup>–</sup> form and the solution pH is 11.5, although for simplicity we still refer as S<sup>2–</sup> below.<sup>8</sup> We first monitored the reaction process between the QD and sulfide by measuring the QD emission properties in the mixed solution as a function of time. As shown in Figure 1a and inset, the QD emission intensity decreases and emission peak red-shifts gradually with mixing time. The solution reaches a steady state after ~150 min when the emission intensity is ~7% of the initial value. Besides reduced intensity, the emission peak of QD-S<sup>2–</sup> shows a red shift of ~14 meV and a broadening in peak width by 5%, as shown in Figure 1b. The absorption spectra of QDs before (denoted as QD) and at 5 h after S<sup>2–</sup> mixing (denoted as QD-S<sup>2–</sup>) are also compared in Figure 1b. The lowest energy (1S) exciton peak (~2.04 eV) as well as high energy excitonic transitions in the QD-S<sup>2–</sup> solution are red-shifted and broadened compared to the QD sample. In

Received: May 19, 2013

Published: July 18, 2013

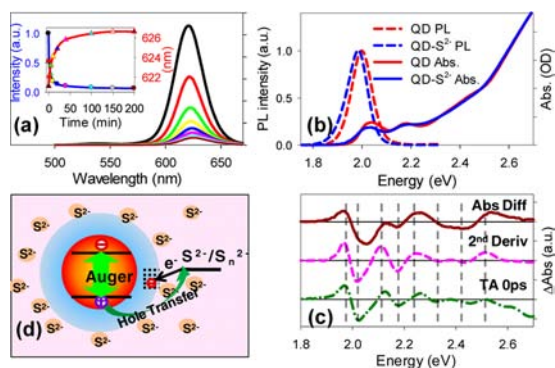


**Figure 1.** (a) Emission spectra of QD solution at different times (0–200 min) after mixing with  $\text{Na}_2\text{S}$  (0.01 M) in dark. Inset: integrated emission intensity (blue line) and peak position (red line) as a function of time. (b) UV–vis absorption (solid lines) and emission spectra (dashed lines) of QDs before (QD) and at 5 h after mixing with  $\text{S}^{2-}$  (QD- $\text{S}^{2-}$ ). (c) Comparison of the absorption difference spectrum between QD- $\text{S}^{2-}$  and QD (brown solid line), 2nd derivative of QD absorption spectrum (pink dashed line) and TA spectra of QDs at 0 ps after 400 nm excitation (green dash-dot line). (d) Schematic diagram showing carrier relaxation pathways: charging of QD surface states by sulfide (black arrow), hole transfer from excited QDs to sulfide (dark green) and Auger recombination (green arrow).

the spectral region above  $\sim 2.7$  eV (data not shown), where featureless bulk-like transitions dominate, the absorption spectra in these samples are nearly identical. These differences can be clearly seen in the absorption difference spectrum between charged and neutral QDs (QD- $\text{S}^{2-}$  – QD) shown in Figure 1c, which exhibits derivative features of exciton bands below  $\sim 2.7$  eV.

Emission quenching and red shift of exciton bands have been reported previously for CdSe QDs in the presence of  $\text{S}^{2-}$ .<sup>8</sup> Emission quenching was attributed to hole transfer from photoexcited QDs to sulfide (see Figure 1d), because sulfide is a well-known hole scavenger in QDSSCs.<sup>8</sup> The  $\text{S}^{2-}$  induced red shift of CdSe QDs was assigned to the formation of  $\text{CdSe}_x\text{S}_{1-x}$  outer layer.<sup>8</sup> Such sulfide corrosion is unlikely in the current QDs because the CdSe core is well protected by multiple shells ( $\sim 2.33$  nm in thickness). In principle, sulfide can bind to the ZnS surface layer (with surface  $\text{Zn}^{2+}$ ) and increases the effective size of QDs. According to an effective mass calculation, the 1S exciton energy decreases by  $\sim 0.3$  meV with one additional ZnS monolayer on the QD studied here, much smaller than the observed 14 meV shift (see SI2<sup>15</sup>). Red-shifted QD absorption peaks can also result from strong coupling between QD levels and adsorbed ligand molecular orbitals.<sup>16</sup> This is also unlikely here because the 1S electron and hole are insulated from the surface adsorbate by multiple shell layers.

Instead, we propose that the observed sulfide induced spectral shift and emission quenching is an indication of QD charging in the sulfide electrolyte. Besides the quantized CB electron and VB hole levels, QDs also have surface states within the band gap. It has been shown that these QD surface states are redox active in electrochemical cells,<sup>17–19</sup> in the presence of chemical reductants,<sup>20,21</sup> or in contact with n-doped semiconductor substrates.<sup>22–24</sup> Sulfide ions can bind strongly to QD surface  $\text{Cd}^{2+}$  or  $\text{Zn}^{2+}$ . Their potential ( $-0.45$  V vs NHE) is not high enough to reduce the CB electron level of QDs used here (estimated to be  $-0.8$  V vs NHE<sup>23</sup>), which can be confirmed by the retention of the 1S exciton feature in the static absorption spectra. This potential is sufficient for removing VB holes,

making sulfides one of the most widely used redox electrolytes in QDSSCs. However, this potential is also sufficient for reducing redox-active mid-gap states, forming charged QDs with surface “spectator” electrons<sup>25</sup> (Figure 1d). These surface charges generate an electric field in the QD, which perturbs the excitonic electron/hole wavefunctions and their optical transitions through Stark effect.<sup>25–28</sup> Charged QDs with red-shifted emission spectra have been reported.<sup>21,22,26</sup> For example, a  $\sim 35$  meV red-shifted emission has been observed for CdSe/ZnS QDs on ITO with estimated 2–3 excess electrons.<sup>22</sup>

It has been well-established that the Stark effect induced spectral change in CdSe QDs can be adequately represented by the second derivative of the absorption spectrum due to electric field induced shifting and mixing of states.<sup>28–30</sup> Indeed, as shown in Figure 1c, the second derivative of the QD absorption spectrum (prior to  $\text{S}^{2-}$  charging) agrees qualitatively with the absorption difference spectrum. Furthermore, Stark effect induced QD spectral change has also been observed in excited QDs.<sup>30</sup> As shown in Figure 1c, the transient absorption (TA) difference spectrum of the QD sample at 0 ps after 400 nm excitation (pulse width  $\sim 150$  fs) is similar to the second derivative of the absorption spectrum of QD and the absorption difference spectrum. At this early delay time, the electric-field of hot electron–hole pairs, generated at high energy levels above the CB and VB edges, modifies the optical transitions at lower energies through Stark effect, giving rise to the derivative like features in the TA spectrum. The similarities of the three spectra shown in Figure 1c provides strong evidence for sulfide induced charging of QDs.

It has been reported that excitons dynamics in charged QDs are significantly altered due to the presence of Auger recombination pathway, in which the electron–hole pair recombines nonradiatively by exciting the extra charges. To probe this effect as well as the expected hole transfer to  $\text{S}^{2-}$ , we studied QD- $\text{S}^{2-}$  and QD samples by both TA spectroscopy and photoluminescence (PL) decay.<sup>23</sup> The TA spectra of both QD and QD- $\text{S}^{2-}$  solutions after 400 nm excitation are shown in Figure S1 and 2a, respectively. The measurements were carried

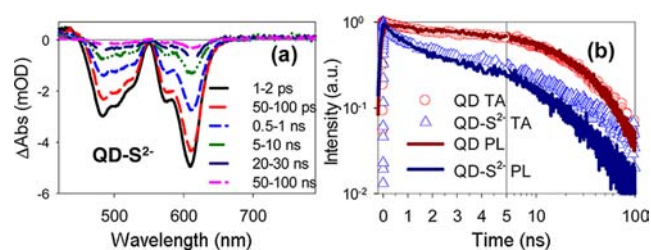


**Figure 2.** (a) TA spectra of QD- $\text{S}^{2-}$  at indicated delay time intervals. (b) TA kinetics at 1S exciton bleach (TA, open symbols) and photoluminescence decay (PL, solid lines) of QD and QD- $\text{S}^{2-}$  solutions. The TA kinetics have been inverted and normalized for better comparison.

out at a low excitation intensity ( $20 \mu\text{J}/\text{cm}^2$ ) to ensure that most excited QDs have only one exciton, which can be confirmed by the lack of a fast decay component in the TA spectra of the QD sample.<sup>31</sup> After 2 ps, when the initially created hot electrons (holes) have relaxed to the CB (VB) edge, the TA spectra show state-filling induced bleach of the 1S exciton band ( $\sim 2.04$  eV) and signals at higher energy positions due to the presence of the 1S exciton.

The 1S exciton bleach recovery and PL decay kinetics of QD and QD- $\text{S}^{2-}$  samples are compared in Figure 2b. For better

comparison with PL decay, the 1S bleach recovery kinetics from TA measurement have been inverted and normalized. For the QD sample, TA and PL decay kinetics agree well with each other, showing an intrinsic half-life time of  $\sim 15$  ns. For QD-S<sup>2-</sup>, both TA and PL kinetics show much faster decay than the QD sample, indicating charging induced exciton quenching in the QD-S<sup>2-</sup> sample. The TA and PL kinetics are similar in the first  $\sim 2$  ns by which time the majority ( $\sim 64\%$ ) of the excited state population has decayed. After that, PL decay kinetics shows a faster decay than the 1S exciton bleach recovery.

Because the 1S exciton TA bleach signal in CdSe QDs is dominated by the state filling of 1S electron level with negligible contribution from the holes, its kinetics reflects the 1S electron depopulation process.<sup>30</sup> The decay rate of the 1S electron TA signal is  $k_{TA} = k_{ETT} + k_{e-h}$ , where  $k_{ETT}$  is the electron trapping/transfer rate for QDs and  $k_{e-h}$  is the 1S electron-hole recombination rate. On the other hand, because the PL intensity is proportional to the concentration of 1S exciton, either electron and hole depopulation processes can lead to PL decay. Therefore, the PL decay kinetics is given by  $k_{PL} = k_{ETT} + k_{e-h} + k_{HTT} = k_{TA} + k_{HTT}$ , where  $k_{HTT}$  is the hole transfer or trapping rate. As shown in Figure 2b, the agreement between TA and PL kinetics of the QD sample indicates negligible hole trapping contributions for these QDs, which is reasonable because the multishell type I structure confines the hole in the CdSe core. For QD-S<sup>2-</sup>, the similar TA and PL kinetics in the first 2 ns suggests that their faster decay compared to free QDs is not caused by hole transfer/trapping process but by additional electron depopulation processes, which can include electron-hole recombination, electron transfer or trapping. Because S<sup>2-</sup> is a hole acceptor, ET from QDs to S<sup>2-</sup> is not expected. Adsorption of S<sup>2-</sup> is also unlikely to enhance electron trapping in this system because of the presence of multiple ZnS shells. Therefore, the most likely reason for the faster TA and PL decay for QD-S<sup>2-</sup> in the first 2 ns is a faster electron-hole recombination process ( $k_{e-h}$ ). It includes the intrinsic decay of uncharged QDs and the additional decay pathways induced by sulfide. Assuming the former remains unchanged, the enhanced electron-hole recombination can be attributed to Auger recombination in charged QDs, as indicated by the green arrow in Figure 1d. This assignment is based on shortened PL lifetime reported in charged QDs prepared by a variety of charging approaches.<sup>17,18,21–24,32</sup> Instead of slow electron-hole radiative decay in neutral QDs, photoexcited electron-hole pairs in charged QDs can recombine nonradiatively with a faster rate by exciting the surface spectator electrons through a Auger recombination process. From the TA decay kinetics in charged and uncharged QDs, a half-life time of  $\sim 1.2$  ns can be estimated for the charging induced Auger recombination process, much shorter than the intrinsic half-life time ( $\sim 15$  ns) for the uncharged QD. A faster PL decay than bleach recovery ( $k_{FL} > k_{TA}$ ) can be clearly observed for QD-S<sup>2-</sup> after  $\sim 2$  ns, indicating the onset of hole removal processes. At 100 ns, most ( $>99\%$ ) of the excited exciton population has been quenched, whereas a relatively larger amount of 1S electrons remains, indicating the near completion of hole filling process within  $\sim 100$  ns.

In QDSSCs, the competition between interfacial ET and intraparticle exciton relaxation determines the electron injection efficiency from photoexcited QDs to semiconductor metal oxide films and thus the device efficiency. To demonstrate the effect of electrolyte charging on electron injection efficiency in QDSSCs, we compare ET processes from these CdSe core/shell QDs to TiO<sub>2</sub> films with and without the presence of S<sup>2-</sup> electrolytes.

With free QDs in solution as a non-ET reference (Ref), the effect of adsorption induced non-ET quenching processes (such as charge and energy transfer between QDs) on films are not accounted for and the measured ET rates and yields represent the upper limit of these values. Although these effects can be accounted for using ZrO<sub>2</sub> films as a reference, it neglects ET activities to these films caused by ET to trap states or sulfide electrolyte induced QD energy shift.<sup>33</sup> Therefore, ZrO<sub>2</sub> reference gives a lower limit of ET rates and yields. As shown in Figure 3a

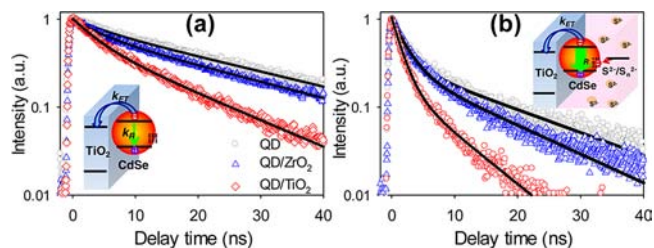


**Figure 3.** PL decay of QDs in solution (gray circles), on ZrO<sub>2</sub> (blue triangles) and TiO<sub>2</sub> (red diamonds) films without (a) and with (b) S<sup>2-</sup> electrolytes. Insets: schematic representation of ET and competing pathways at QD/TiO<sub>2</sub> interfaces.

and b, QDs on TiO<sub>2</sub> show a faster decay than on ZrO<sub>2</sub> and in solution, confirming ET from QDs to TiO<sub>2</sub>. In the presence of S<sup>2-</sup> electrolyte, QDs on both ZrO<sub>2</sub> and TiO<sub>2</sub> films and in solution have much shorter exciton lifetimes due to electrolyte charging induced fast Auger recombination in QDs. These PL decay kinetics can be well fitted by biexponential function (as shown in black line), from which a half-life time  $\langle\tau\rangle_{1/2}$  can be determined (listed in SI4). From the half-life times of QDs on TiO<sub>2</sub> and in Ref, the average ET rates  $k_{ET}$  from QDs to TiO<sub>2</sub> can be determined to be  $\sim 0.09$ – $0.11$  ns<sup>-1</sup> (without S<sup>2-</sup>) and  $0.19$ – $0.22$  ns<sup>-1</sup> (with S<sup>2-</sup>), respectively, using  $k_{ET} = 1/\langle\tau_{1/2}\rangle_{TiO_2} - 1/\langle\tau_{1/2}\rangle_{Ref}$ . Together with the QD intrinsic decay rate,  $k_R = 1/\langle\tau_{1/2}\rangle_{Ref}$ , the electron injection efficiency can be estimated by  $\eta_{inj} = k_{ET}/(k_{ET} + k_R)$ . The electron injection efficiency is 48–60% for QDs on TiO<sub>2</sub> films without S<sup>2-</sup> electrolyte solution. In the presence of S<sup>2-</sup> solution, the electron injection efficiency decreases to  $\sim 29$ – $33\%$ , despite an increase in injection rate. The reduced electron injection efficiency is attributed to electrolyte charging induced Auger recombination in QDs, which competes efficiently with the interfacial ET process. The increase in injection rate is likely caused by changes in the energetics of QDs and TiO<sub>2</sub> films in the presence sulfide electrolyte.<sup>33</sup>

QDSSCs based on TiO<sub>2</sub> nanocrystalline thin films sensitized by core-only CdSe QDs have been extensively studied.<sup>5–7,34,35</sup> Interfacial ET times from CdSe QDs to TiO<sub>2</sub> in the absence of redox electrolytes are typically several to hundreds of picoseconds.<sup>6,11,13,14</sup> Considering the relatively long intrinsic exciton lifetime in such QDs measured in solutions or on insulating films ( $\sim 10$  ns),<sup>7,14,15</sup> efficient carrier injection and high absorbed-photon-to-charge-efficiency (APCE) values in QDSSCs were expected. The reported APCE values for QDSSCs based on core-only QDs are often small ( $< \sim 45\%$ ).<sup>6,7,11,34–36</sup> These QDs should also be charged in working devices due to the presence of sulfide and other redox electrolytes. The Auger recombination rate in charged core-only CdSe QDs should be faster than that in multishell QDs studied here, since the former usually have more surface trapping sites and the spectator electrons interact more strongly with the excitons. On the basis of the previously

reported biexciton lifetime in core-only CdSe QDs (10s of ps)<sup>31</sup> and the measured Auger recombination lifetime in charged CdSe core/multishell QDs, the Auger recombination time in charged core-only CdSe QDs can be assumed to be tens to hundreds of picoseconds. This exciton Auger recombination lifetime is comparable with ET time to TiO<sub>2</sub>, which would lead to low electron injection efficiency in these QDSSCs (Figure 3b inset). It is likely that the reduced electron injection efficiency caused by QD charging and the reported interfacial charge recombination loss are two of the main reasons for the observed low APCE values and power conversion efficiencies in CdSe QDSSCs.<sup>8,34,37,38</sup> Interestingly, compared to single component CdSe/TiO<sub>2</sub> QDSSCs, similar devices with ZnS or CdTe overlayer coating,<sup>35,36</sup> CdS and CdSe cosensitization,<sup>38,39</sup> or multilayer CdSe<sup>40</sup> have exhibited much higher APCE values. Besides the reported retardation of charge recombination process, a reduction in Auger recombination rate in charged QDs may also be in part responsible for the improved efficiency. These multilayer structures decrease the interaction of excitons with the surface spectator electrons located at QD-electrolyte interface, thus reducing Auger recombination rate and enhancing the electron injection efficiency.

In conclusion, with steady-state and time-resolved absorption and emission spectroscopic techniques, we show that CdSe core/shell QDs are charged in the presence of sulfide electrolytes, and exciton lifetimes are shortened in charged QDs due to fast Auger recombination process (~1.2 ns). When this charging induced Auger recombination time is comparable with interfacial ET time, the efficiency of charge separation decreases, degrading the performance of QD-based photovoltaic and photocatalytic devices. We believe that this is a key efficiency reducing factor that has often been overlooked in these QD based devices. This charging effect should be present for most colloidal QDs and nanostructures in redox active media, including QDSSCs with redox electrolytes and QD-based photocatalytic solutions with sacrificial electron donors, as long as the chemical potentials of the redox couples are located above the surface trap states in QDs. Our findings also highlight a fundamental difference between QDs and molecular dyes in redox reactions, i.e., the presence redox active mid-gap states can lead to the formation of charged QDs with significantly shortened excited state lifetimes.

## ■ ASSOCIATED CONTENT

### ● Supporting Information

Experimental details, effective mass calculation and fitting parameters. This material is available free of charge via the Internet at <http://pubs.acs.org>.

## ■ AUTHOR INFORMATION

### Corresponding Author

tlian@emory.edu

### Notes

The authors declare no competing financial interest.

## ■ ACKNOWLEDGMENTS

The authors gratefully acknowledge the financial support from the National Science Foundation (CHE-1212907).

## ■ REFERENCES

- (1) Kamat, P. V.; Tvrđy, K.; Baker, D. R.; Radich, J. G. *Chem. Rev.* **2010**, *110*, 6664.
- (2) Nozik, A. J.; Beard, M. C.; Luther, J. M.; Law, M.; Ellingson, R. J.; Johnson, J. C. *Chem. Rev.* **2010**, *110*, 6873.
- (3) Semonin, O. E.; Luther, J. M.; Choi, S.; Chen, H.-Y.; Gao, J.; Nozik, A. J.; Beard, M. C. *Science* **2011**, *334*, 1530.
- (4) Tisdale, W. A.; Williams, K. J.; Timp, B. A.; Norris, D. J.; Aydil, E. S.; Zhu, X.-Y. *Science* **2010**, *328*, 1543.
- (5) Tachibana, Y.; Akiyama, H. Y.; Ohtsuka, Y.; Torimoto, T.; Kuwabata, S. *Chem. Lett.* **2007**, *36*, 88.
- (6) Robel, I.; Subramanian, V.; Kuno, M.; Kamat, P. V. *J. Am. Chem. Soc.* **2006**, *128*, 2385.
- (7) Kongkanand, A.; Tvrđy, K.; Takechi, K.; Kuno, M.; Kamat, P. V. *J. Am. Chem. Soc.* **2008**, *130*, 4007.
- (8) Chakrapani, V.; Baker, D.; Kamat, P. V. *J. Am. Chem. Soc.* **2011**, *133*, 9607.
- (9) Hod, I.; González-Pedro, V.; Tachan, Z.; Fabregat-Santiago, F.; Mora-Seró, I.; Bisquert, J.; Zaban, A. *J. Phys. Chem. Lett.* **2011**, 3032.
- (10) Shalom, M.; Tachan, Z.; Bouhadana, Y.; Barad, H.-N.; Zaban, A. *J. Phys. Chem. Lett.* **2011**, *2*, 1998.
- (11) Tvrđy, K.; Frantsuzov, P. A.; Kamat, P. V. *Proc. Natl. Acad. Sci. U.S.A.* **2011**, *108*, 29.
- (12) Židek, K.; Zheng, K.; Ponseca, C. S.; Messing, M. E.; Wallenberg, L. R.; Chábera, P.; Abdellah, M.; Sundström, V.; Pullerits, T. *J. Am. Chem. Soc.* **2012**, *134*, 12110.
- (13) Watson, D. F. *J. Phys. Chem. Lett.* **2010**, *1*, 2299.
- (14) Robel, I.; Kuno, M.; Kamat, P. V. *J. Am. Chem. Soc.* **2007**, *129*, 4136.
- (15) Zhu, H.; Song, N.; Lian, T. *J. Am. Chem. Soc.* **2010**, *132*, 15038.
- (16) Frederick, M. T.; Amin, V. A.; Cass, L. C.; Weiss, E. A. *Nano Lett.* **2011**, *11*, 5455.
- (17) Galland, C.; Ghosh, Y.; Steinbruck, A.; Sykora, M.; Hollingsworth, J. A.; Klimov, V. I.; Htoon, H. *Nature* **2011**, *479*, 203.
- (18) Qin, W.; Guyot-Sionnest, P. *ACS Nano* **2012**, *6*, 9125.
- (19) Weaver, A. L.; Gamelin, D. R. *J. Am. Chem. Soc.* **2012**, *134*, 6819.
- (20) Rinehart, J. D.; Weaver, A. L.; Gamelin, D. R. *J. Am. Chem. Soc.* **2012**, *134*, 16175.
- (21) Bang, J.; Chon, B.; Won, N.; Nam, J.; Joo, T.; Kim, S. *J. Phys. Chem. C* **2009**, *113*, 6320.
- (22) Yalcin, S. E.; Yang, B.; Labastide, J. A.; Barnes, M. D. *J. Phys. Chem. C* **2012**, *116*, 15847.
- (23) Song, N.; Zhu, H.; Liu, Z.; Huang, Z.; Wu, D.; Lian, T. *ACS Nano* **2013**, *7*, 1599.
- (24) Jin, S.; Song, N.; Lian, T. *ACS Nano* **2010**, *4*, 1545.
- (25) Franceschetti, A.; Zunger, A. *Phys. Rev. B* **2000**, *62*, R16287.
- (26) Early, K. T.; Sudeep, P. K.; Emrick, T.; Barnes, M. D. *Nano Lett.* **2010**, *10*, 1754.
- (27) Wang, L. W. *J. Phys. Chem. B* **2001**, *105*, 2360.
- (28) Sacra, A.; Norris, D. J.; Murray, C. B.; Bawendi, M. G. *J. Chem. Phys.* **1995**, *103*, 5236.
- (29) Norris, D. J.; Sacra, A.; Murray, C. B.; Bawendi, M. G. *Phys. Rev. Lett.* **1994**, *72*, 2612.
- (30) Klimov, V. I. *J. Phys. Chem. B* **2000**, *104*, 6112.
- (31) Klimov, V. I.; Mikhailovsky, A. A.; McBranch, D. W.; Leatherdale, C. A.; Bawendi, M. G. *Science* **2000**, *287*, 1011.
- (32) Yalcin, S. E.; Labastide, J. A.; Sowle, D. L.; Barnes, M. D. *Nano Lett.* **2011**, *11*, 4425.
- (33) Greenwald, S.; Ruhle, S.; Shalom, M.; Yahav, S.; Zaban, A. *Phys. Chem. Chem. Phys.* **2011**, *13*, 19302.
- (34) Lee, H. J.; Yum, J.-H.; Leventis, H. C.; Zakeeruddin, S. M.; Haque, S. A.; Chen, P.; Seok, S. I.; Grätzel, M.; Nazeeruddin, M. K. *J. Phys. Chem. C* **2008**, *112*, 11600.
- (35) Lee, H.; Wang, M.; Chen, P.; Gamelin, D. R.; Zakeeruddin, S. M.; Grätzel, M.; Nazeeruddin, M. K. *Nano Lett.* **2009**, *9*, 4221.
- (36) Shen, Q.; Kobayashi, J.; Diguna, L. J.; Toyoda, T. *J. Appl. Phys.* **2008**, *103*, 084304.
- (37) Barea, E. M.; Shalom, M.; Giménez, S.; Hod, I.; Mora-Seró, I. n.; Zaban, A.; Bisquert, J. *J. Am. Chem. Soc.* **2010**, *132*, 6834.
- (38) Yu, X.-Y.; Liao, J.-Y.; Qiu, K.-Q.; Kuang, D.-B.; Su, C.-Y. *ACS Nano* **2011**, *5*, 9494.
- (39) Lee, Y.-L.; Lo, Y.-S. *Adv. Funct. Mater.* **2009**, *19*, 604.
- (40) Shalom, M.; Buhbut, S.; Tirosh, S.; Zaban, A. *J. Phys. Chem. Lett.* **2012**, *3*, 2436.